2008

A Statistical Model for Linking Field and Laboratory Exposure Results for a Model Coating

Iliana Vaca-Trigo
Iowa State University

William Q. Meeker
Iowa State University, wqmeeker@iastate.edu

Follow this and additional works at: http://lib.dr.iastate.edu/stat_las_preprints

Part of the Statistics and Probability Commons

A Statistical Model for Linking Field and Laboratory Exposure Results for a Model Coating

Abstract

Today's manufacturers need accelerated test (AT) methods that can usefully predict service life in a timely manner. For example, automobile manufacturers would like to develop a three-month test to predict 10-year field reliability of a coating system (an acceleration factor of 40). Developing a methodology to simulate outdoor weathering is a particularly challenging task and most previous attempts to establish an adequate correlation between laboratory tests and field experience has met with failure. Difficulties arise, for example, because the intensity and the frequency spectrum of ultraviolet (UV) radiation from the Sun are highly variable, both temporally and spatially and because there is often little understanding of how environmental variables affect chemical degradation processes.

This paper describes the statistical aspects of a cooperative project being conducted at the U.S. National Institute of Standards and Technology (NIST) to generate necessary experimental data and the development of a model relating cumulative damage to environmental variables like UV spectrum and intensity, as well as temperature and relative humidity. The parameters of the cumulative damage are estimated from the laboratory data. The adequacy of the model predictions are assessed by comparing with specimens tested in an outdoor environment for which the environmental variables were carefully measured.

Disciplines

Statistics and Probability

A Statistical Model for Linking Field and Laboratory Exposure Results for a Model Coating

Iliana Vaca-Trigo and William Q. Meeker

Department of Statistics, Iowa State University, Ames, IA 50011-1210

Abstract

Today's manufacturers need accelerated test (AT) methods that can usefully predict service life in a timely manner. For example, automobile manufacturers would like to develop a three-month test to predict 10-year field reliability of a coating system (an acceleration factor of 40). Developing a methodology to simulate outdoor weathering is a particularly challenging task and most previous attempts to establish an adequate correlation between laboratory tests and field experience has met with failure. Difficulties arise, for example, because the intensity and the frequency spectrum of ultraviolet (UV) radiation from the Sun are highly variable, both temporally and spatially and because there is often little understanding of how environmental variables affect chemical degradation processes.

This paper describes the statistical aspects of a cooperative project being conducted at the U.S. National Institute of Standards and Technology (NIST) to generate necessary experimental data and the development of a model relating cumulative damage to environmental variables like UV spectrum and intensity, as well as temperature and relative humidity. The parameters of the cumulative damage are estimated from the laboratory data. The adequacy of the model predictions are assessed by comparing with specimens tested in an outdoor environment for which the environmental variables were carefully measured.

Key words: Cumulative damage, Nonlinear regression, Photodegradation, Prediction, Reliability, Weathering

1. Introduction

1.1 Background

Photodegradation, caused by UV radiation, is a primary cause of failure for paints and coatings (as well as all other products made from organic materials) exposed to sunlight. Other variables that affect degradation rates include temperature and humidity. Manufacturers of such paints and coatings have had difficulty in using laboratory tests to predict field experience for their products. Historically, most of the laboratory tests attempt to accelerate time by "speeding up the clock." This is done by increasing the average levels of experimental factors like UV radiation, temperature, and humidity and cycling these experimental factors more rapidly than what is seen in actual use, in an attempt to simulate and accelerate outdoor aging. Such experiments violate the basic rules of good experimental design. For example, varying important factors together tends to confound the effects of the factors. Also, levels of the accelerating variables that are too high may induce new failure modes. For these reasons, such accelerated tests provide little fundamental understanding of the underlying degradation mechanisms and conclusions from them can be seriously incorrect. Because experience has shown that the results of these tests are unreliable, standard product evaluation for paints and coatings still requires outdoor testing in places like Florida (where it is hot and humid) and Arizona (where it is hot and dry). Outdoor testing, however, is costly and takes too much time.

Martin, Saunders, Floyd, and Wineburg (1996) and Martin (1999) provide a detailed description of issues relating to prediction of service life (SL) for paints and coatings. In general the accelerated test methodology for photodegradation is much more complicated than those typically used for electronic and mechanical devices (e.g., as described in Nelson 1990 and Chapters 18-21 Meeker and Escobar 1998). This is because of the complicated chemical/physical failure mechanisms involved and the highly-variable use environment.

1.2 Motivation

Accelerated test (AT) methods have proven to be useful for predicting the SL of materials in certain applications. These range from jet engine turbine disk materials to highly

sophisticated microelectronics [these successful applications are described, for example, in Gillen and Mead (1980), Joyce et al. (1985), Starke et al. (1996), and the many examples cited in Nelson (1990)]. In other areas of application, however, AT methods often yield predictions that do not correlate well with field data. This is particularly true for products exposed to outdoor weathering, such as organic paints and coatings used on automobiles, bridges, buildings and other outdoor structures [e.g., Martin et al. (1996) and Wernstål and Carlsson (1997)]. For this reason, conventional laboratory AT methods are not trusted for outdoor-use products and potential users of such tests have been forced to rely on expensive, time-consuming outdoor testing.

Traditional applications in reliability and service life prediction based on accelerated test results, involve chemical degradation that is accelerated by increasing variables like temperature, humidity, and current density or voltage stress, using statistical models that are motivated by knowledge from physical chemistry. The research described in this paper is a natural extension of previous work in this area to the more complicated area of photodegradation.

2. Experimental Data

Degradation (or damage) at time t, denoted by Đ(t), usually depends on environmental variables like UV, temperature, and relative humidity that vary *over time*. Laboratory tests are conducted in well-controlled environments, usually holding these variables constant (although in other experiments such variables are purposely changed during an experiment, as in step-stress accelerated tests). Interest often centers, however, on life in a variable environment.

2.1 Time Scale for Photodegradation

It is important to choose an appropriate time scale to describe the behavior of a failure mechanism (e.g., number of miles for an automobile engine bearing or number of cycles for fatigue caused by cyclic stress). The appropriate time scale for photodegradation is photon dosage. In our data sets, dosage is given in units of KJ/m^2/nm and is a number that is proportional to the number of photons absorbed into the experimental specimens.

2.2 Indoor Data

In the current phase of the NIST research program, the goal has been to develop a service life prediction methodology using as a simple model, a crosslinked epoxy amine coating system. The methodology described in this paper is being developed, however, to allow easy generalization to service life prediction of other types of materials that will be exposed to outdoor weathering.

Researchers at NIST have conducted weathering experiments in both the indoor laboratory, as well as in outdoor exposure facilities. Indoor data are being taken in temperature/humidity-controlled chambers illuminated by controlled UV light from the NIST Sphere [described in Martin et al. (1999) and Chin et al. (2000)].

Indoor data received from NIST consist of the variables:

- Specimen Number (SA) identifying the testing chamber number and a number of a particular specimen within the chamber.

- Damage number (DA) for four peaks in the measured FTIR spectra. The heights of the peaks correspond to the amount of particular chemical products and these were measured systematically, over time, and have units cm^{-1}. One of the studied damage numbers was the peak at 1510 $cm^{-1,}$ which corresponds to benzene ring mass loss. Other peaks being used as potentially useful responses include 1250 cm^{-1} (aromatic C-O), 1658 cm^{-1} (oxidation products), and 2925 cm^{-1} (CH mass loss).

- Bandpass Filter (FI) is the center wavelength in nanometers (nm) of the bandpass filter used in exposure. Table 1 Bandpass Filter characteristics also gives the range of the bandpass filters.

Table 1 Bandpass Filter characteristics

Range		Nominal Filter Midpoint
303 nm	309 nm	306 nm
320 nm	332 nm	326 nm
334 nm	372 nm	353 nm
372 nm	532 nm	452 nm

- Neutral Density (DE) is the nominal transmittance rate of a neutral density filter ranging from 0% to 100%.

- Temperature (temp) in Celsius.

- Relative Humidity (RH) which ranges from 0% to 100%.

- DOSAGE$_{Tot}$, as part of the indoor data, is a metric proportional the total number of photons absorbed into the degrading material.

- DAMAGE values are the responses and measure the photolytic part of the chemical damage to the test specimens.

- Wall Clock is the real clock time when the data is recorded, as the number of days since January 1, 1900.

Table 2 Experimental Variables and Levels

Variable	Units	Levels
Damage Number (DA)	cm^{-1}	1250,1510, 1658, 2925
Bandpass Filter (FI)	nm	306, 326, 353, 452
Neutral Density (DE)	%	10, 40, 60, 100
Temperature (temp)	^{o}C	25, 35, 45, 55
Humidity (RH)	%	0, 25, 50, 75

Table 2 shows the levels of the experimental variables in the Indoor data. Not all combinations of humidity and temperature levels data were available at the time of the analysis provided here. Table 3 shows the combinations that we used.

Table 3 Available data

RH temp	0%	25%	50%	75%
25°C	x			
35°C	x	✓	✓	✓
45°C	x	✓	✓	x
55°C	x	x	x	✓

	Data not available
✓	Data used for modeling
x	Data not used for modeling

2.3 Outdoor damage data

Outdoor exposure data on specimens made of the same material were also collected at NIST. For outdoor specimens, damage is typically measured after every few days of exposure and this information is recorded in addition to spectral irradiance and weather data (temperature and humidity). Although there was no control of experimental variables for the outdoor data, temperature, humidity, and solar data were recorded, as described in the next subsection. Specimens in the outdoor were grouped by date, with 18 groups and four replicates for each group.   Each group was exposed across different months, therefore temperature and humidity change from group to group. The outdoor data will allow us to check our predictive model. This will be done by generating damage predictions based on the model derived from the indoor data. To do this, the indoor model is driven by the outdoor weather data to compute predictions that can be compared with the corresponding actual outdoor damage.

2.4 Outdoor weather data

SOLARNET, a solar UV data network, stores spectral irradiance data with a 12-minute resolution as well as climatological data (temperature, relative humidity, etc) as 1 minute averages [described in Kaetzel, (2001)].

3.   Analysis and Initial Modeling

Initially, extensive graphical analyses of damage versus dosage paths plots were conducted to get a good understanding of the data and possible relations among variables in the data

set. Plots of empirically estimated acceleration factors provided insight on the effects that experimental explanatory variables have on the response.

Acceleration factors are commonly used to describe the effect that accelerating variables or other experimental variables have on lifetime or degradation rates. Acceleration factors can be expressed as the ratio of life at "fixed test conditions" to life at "higher test conditions". Acceleration factor plots were examined for temperature, humidity, and the different UV radiation band pass filters.

3.1 Data Cleaning

An important phase of modeling is looking at the raw data to identify strange patterns, outliers or other data anomalies that could affect the modeling efforts and possibly result in unreliable estimates. Even though data were collected under a controlled environment using sophisticated analytical devices to assure the accuracy of the data, exhaustive use of graphical assessment procedures helped to identify some potential problems. The root cause for all such problems was determined and appropriate adjustments were made to the data. For example, we detected a sharp drop in the damage rate for samples at 45$^{\text{o}}$C and 75%RH. The root cause for this problem was the failure of an integrated circuit chip in the environmental controllers that caused the samples in one of the chambers to be overheated for a period of time. Similar problems were identified at 55$^{\text{o}}$C and 25%RH as well as at 55$^{\text{o}}$C and 50%RH. Those specimens that were subjected to this overheating were not used in the modeling process. Also, data from the bandpass filter with nominal midpoint of 353 nm did not agree with the data from the other bandpass filters when fitting a model to estimate the effect of wavelength on damage rates. For this reason, these data were also ignored in the modeling.
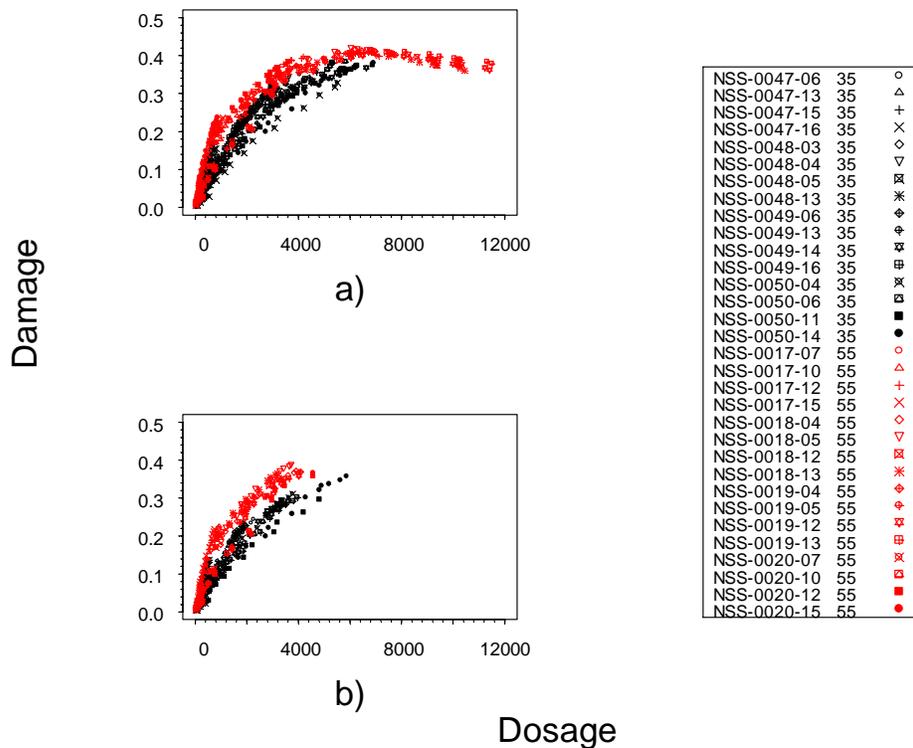
NSS-0047-06	35	○
NSS-0047-13	35	△
NSS-0047-15	35	+
NSS-0047-16	35	×
NSS-0048-03	35	◇
NSS-0048-04	35	▽
NSS-0048-05	35	⊠
NSS-0048-13	35	✳
NSS-0049-06	35	◈
NSS-0049-13	35	⊕
NSS-0049-14	35	⊠
NSS-0049-16	35	⊞
NSS-0050-04	35	⊠
NSS-0050-06	35	◰
NSS-0050-11	35	■
NSS-0050-14	35	●
NSS-0017-07	55	○
NSS-0017-10	55	△
NSS-0017-12	55	+
NSS-0017-15	55	×
NSS-0018-04	55	◇
NSS-0018-05	55	▽
NSS-0018-12	55	⊠
NSS-0018-13	55	✳
NSS-0019-04	55	◈
NSS-0019-05	55	⊕
NSS-0019-12	55	⊠
NSS-0019-13	55	⊞
NSS-0020-07	55	⊠
NSS-0020-10	55	◰
NSS-0020-12	55	■
NSS-0020-15	55	●

Figure 1   Illustration of data cleaning for the FTIR peak at 1658cm^{-1} for units exposed with 326 nm nominal bandpass filter midpoint and 75%RH. a) Original data paths. b) Data paths after deleting outliers and increasing tails.

Another potential data complication is   a change of direction of the degradation path. For example, Figure 1a shows that the FTIR peak at 1658cm^{-1} increases until dosage reaches approximately 4×10^3 KJ/m^2/nm, after which the degradation paths begin to decrease. This behavior is thought to be caused by physical and chemical changes in the specimens. Because the turning point is far beyond the definition of failure, modeling beyond the turning point is not needed. Thus we cut increasing/decreasing tails after the turning point for those cases where degradation paths changed direction. In addition specimens at 0%RH were used only in the preliminary stages to understand data behavior. Because 0%RH is outside of the region of interest and because there was no apparent simple model to connect these "dry" results with the units run with humidity, the 0%RH data were not used in our modeling.

3.2 Initial Modeling

The data that have been analyzed to date seem to be consistent with both first-order and second-order kinetic models. Over the dosage range of interest, (that is up to the point where $Đ(t)$ has reached a failure state) we have found, empirically, that the simple parsimonious functional form

$$Đ(t) = [Đ(\infty)\text{-}Đ(0)]\left[\frac{\exp(z)}{1+\exp(z)}\right] \qquad (1)$$

$$z = \frac{\log\big[d(t)\big] - \mu}{\sigma} \qquad (2)$$

fits the data well for all FTIR peaks of interest and at *all* combinations of the experimental factors for which we have received data. Here $d(t)$ is the effective total dosage. Also, $Đ(0)$ is the standardized level of damage at time 0 and $Đ(\infty)$ is the long-term asymptote; while μ, and σ are parameters that describe the location and steepness of the damage curve, respectively. In the overall model, time-scaling factor $\exp(\mu)$ will be a function of the environment and additional unknown parameters. When fitting data to a single path, if the asymptote cannot be estimated from the data (because the path has not begun to level off sufficiently), a good fit to the data can be obtained, without loss of generality, by setting $Đ(\infty)$ to a safe lower bound (upper bound) on the asymptote when the damage variable is decreasing (increasing). When we fit data to the overall model, we will be able to "borrow strength" from paths at other conditions where the asymptote can be identified. For the NIST data on the epoxy material under study suggest that there is, approximately, a common asymptote for each FTIR peak, independent of the experimental conditions and we assume this in the overall model.

As an aid in model identification, a plot of an acceleration factor versus a particular experimental variable can be generated by fitting the model in equations (1) and (2) with a common value of σ and a different value of μ for each level of experimental variable. The acceleration factor at a given test level of the variable, relative to a specified reference level, is

$$AF(\text{test,reference}) = \frac{\exp\left(\mu_{\text{test}}\right)}{\exp\left(\mu_{\text{reference}}\right)}$$

The acceleration factors for the different levels of the experimental variables can be plotted in a manner such that the points should fall roughly along a straight line if the hypothesized model is adequate.

4. Model for the Effect of UV Radiation on Photodegradation

Many of the ideas in this section are based on early research into the effects of light on photographic emulsions (e.g., James 1977) and the effect that UV exposure has on causing skin cancer (e.g., Blum 1959).

4.1 Model for Total Effective UV dosage

As described in Martin et al. (1996), the appropriate time scale for photodegradation is D_{Tot}, the total *effective* UV dosage. Intuitively, this total effective dosage can be thought of as the number of photons absorbed into the degrading material *and that cause chemical change*. The total *effective* UV dosage at real time t can be computed from

$$D_{\text{Tot}}(t) = \int_0^t D_{\text{Inst}}(\tau)d\tau \tag{3}$$

where the instantaneous *effective* UV dosage D_{Inst} is

$$D_{\text{Inst}}(\tau) = \int_{\lambda_1}^{\lambda_2} D_{\text{Inst}}(\tau,\lambda)d\lambda = \int_{\lambda_1}^{\lambda_2} E_0(\tau,\lambda)\left\{1-\exp\left[-A(\lambda)\right]\right\}\phi(\lambda)d\lambda. \tag{4}$$

Here E_0 is the spectral irradiance of the light source (both artificial and natural light sources have mixtures of light at different wavelengths, denoted by λ), $[1 - \exp(-A(\lambda))]$ is the spectral absorbance of the material being exposed (damage is caused only by photons that are absorbed into the material), and $\phi(\lambda)$ is a quasi quantum efficiency (QQE) of the absorbed radiation (allowing for the fact that photons at shorter wavelengths have higher energy and thus a higher probability of causing damage). The functions in the integrand of equation (4) can either be measured directly (E_0 and A) or estimated from experimental data ($\phi(\lambda)$). The definition of dosage in (4) differs from the dosage in our data (as

9

described in section 2.2) because the QQE function is unknown and needs to be identified from the experimental data.

4.2 Intensity effects and reciprocity

The intuitive idea behind reciprocity in photodegradation is that the time to reach a certain level of degradation is inversely proportional to rate at which photons reach the material being degraded. Reciprocity failure occurs when the coefficient of proportionality changes with light intensity.

Although reciprocity provides an adequate model for some degradation processes (particularly when the dynamic range of intensities used in experimentation and actual applications is not too large) numerous examples have been reported in which there is reciprocity failure (e.g., Blum 1959 and James 1977). Light intensity can be affected by filters. Sunlight is filtered by the earth's atmosphere. In laboratory experiments, neutral density filters are used to reduce the amount of light passing to specimens (without having an important effect on the wavelength spectra), providing an assessment of the degree of reciprocity failure.

Reciprocity also implies that the effective time of exposure is

$$d(t) = \text{CF} \times \text{D}_{\text{Tot}}(t) = \text{CF} \times \left[\int_0^t \int_{\lambda_1}^{\lambda_2} \text{D}_{\text{Inst}}(\tau, \lambda) d\lambda d\tau \right] \tag{5}$$

where CF is an acceleration or deceleration factor for UV intensity. For example, commercial outdoor test exposure sites use mirrors to achieve, say "5 Suns" *acceleration* or $\text{CF} = 5$. A 50% neutral density filter in a laboratory experiment will provide *deceleration* corresponding to $\text{CF} = 0.50$.

When there is evidence of reciprocity failure, the effective time of exposure is often modeled by

$$d(t) = (\text{CF})^p \times \text{D}_{\text{Tot}}(t) = (\text{CF})^p \times \left[\int_0^t \int_{\lambda_1}^{\lambda_2} \text{D}_{\text{Inst}}(\tau, \lambda) d\lambda d\tau \right]. \tag{6}$$

where p is known as the Schwarzschild coefficient. This model has been shown to fit data well and experimental work in the photographic literature (e.g., James, 1966) suggests that

when there is reciprocity failure, the value of p does not depend on wavelength λ. A statistical test of $p = 1$ can be used to assess the reciprocity assumption.

For the NIST data on the epoxy material under study, there is no evidence of reciprocity failure. Thus, for this material, we expect to be able to use $p = 1$. Our model is, however, general enough to allow for reciprocity failure. Therefore, for modeling purposes, averages of damage values for specimens exposed at same conditions but different neutral density filters were used instead of individual paths.

Following other work in the area of photodegradation (e.g., Miller at al. 2002), we will assume a simple log-linear model for QQE. That is,

$$\phi(\lambda) = \exp(\beta_0 + \beta_1 \lambda).$$

The integral in equation (5) and subsequent integrals over wavelength are typically taken over the UV-B band (280—315 nm), as this is the range of wavelengths over which both $\phi(\lambda)$ and $E_0(\lambda, t)$ are importantly different from 0. Longer wavelengths (in the UV-A band) are not terribly harmful so that $\phi(\lambda) \approx 0$. Shorter wavelengths (in the UV-C band) have more energy, but are absorbed by ozone in the atmosphere so that $E_0(\lambda, t) \approx 0$.

An example of an acceleration factor versus wavelength plot, is shown in upper plot of Figure 2. The horizontal lines indicate the band pass filter width. These lines exhibit a log-linear relation for QQE except for observations corresponding to BP filter 353. Because observations from BP filter 353 were not consistent (in terms of our estimated QQY function) with the observations from the other BP filters, the 353 BP data were not used in the estimation of the parameters of the model.

The lower plot in Figure 2 shows degradation paths of observed damage averaged over all specimens under experimental 35°C, 25%RH, 1250 cm^{-1} FTIR peak and a particular nominal bandpass filter midpoint. Different symbols were used to identify the bandpass filters. Filled marks and continuous lines identified data that were used in the modeling while dashed lines and open marks were used to represent data that were available, but not used in the modeling as explained in Section 3.1. Figure 2 shows that, all other things being equal, wavelength has an effect on damage that tends to be stronger at shorter wavelengths.
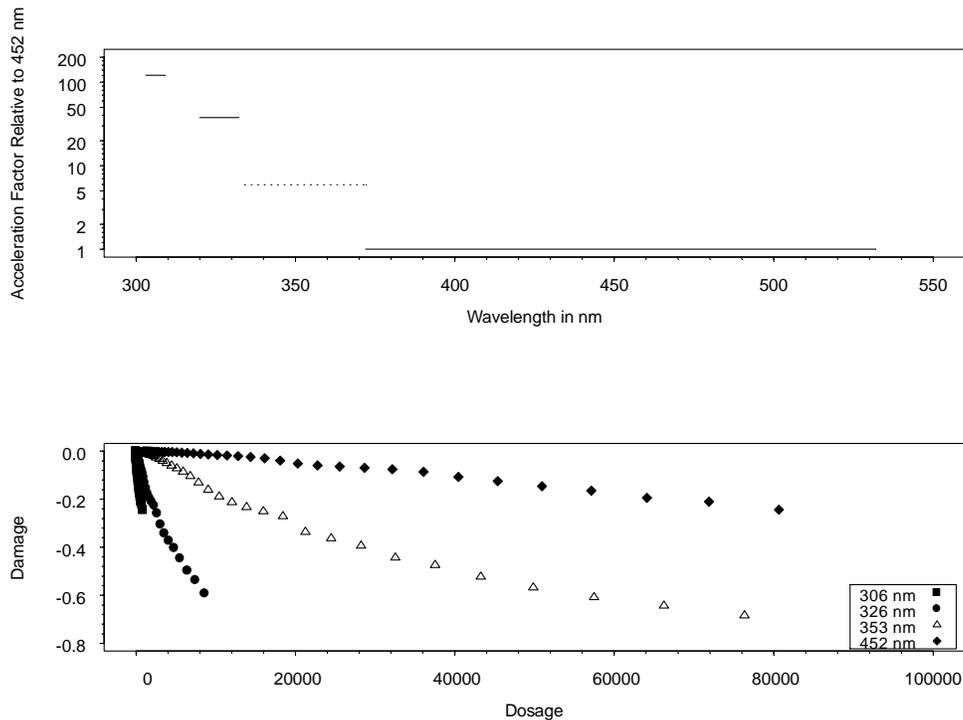
Figure 2 Quantum Yield Model Check for the 1250 cm^{-1} FTIR peak for specimens exposed at 35°C and 25% RH

Implicit in the model in equation (4) is the assumption of additivity. Additivity implies, in this setting, that the photoeffectiveness of a source is equal to the sum of the effectiveness of its spectral components. Experimental results obtained by NIST researchers support additivity in photodegradation of organic materials that have been studied to date.

5.   Model for Other Experimental Variables

5.1 Temperature Effects

As described, for example, by Meeker and Escobar (1998, Chapter 18), the Arrhenius equation for the reaction rate $\mathcal{R}$ can be written as

$$\mathcal{R}(\text{temp}) = \gamma_0 \exp\left(\frac{-E_a}{R \times \text{temp } \mathbf{K}} \right)$$

12

where temp **K** is temperature Kelvin, R is the gas constant ($R = 8.31447 \text{ J} \times \text{K}^{-1} \times \text{mol}^{-1}$),
E_a is a quasi activation energy and γ_0 is a constant specific to a product or material.
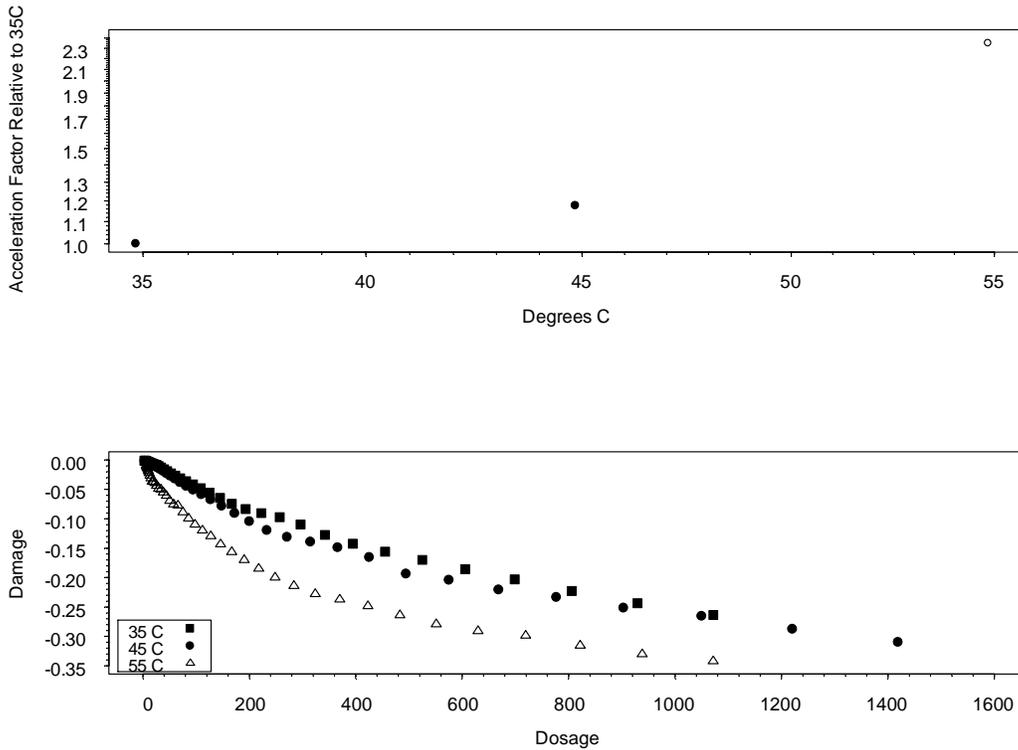

Figure 3 Arrhenius Model check for the 1250 cm^{-1} FTIR peak, specimens exposed to 306 nm nominal bandpass filter midpoint and 25%RH

The Arrhenius rate reaction model can be used to scale time (or dosage) in the usual manner and the upper plot in Figure 3 shows the acceleration factor versus temperature, plotted relative to 35°C and accelerated temperatures from 35°C to 55°C. Because 25°C data were not available for all humidity levels, for sake of consistency 35°C was used as a basis level for calculating acceleration factors. Temperature was plotted on an Arrhenius scale while acceleration factor was plotted on a logarithmic scale. The acceleration factor for a temperature of 45°C is approximately 1.2. This means that the life at the use level of 35°C is approximately 1.2 times longer than the life at 45°C.   The bottom plot in Figure 3 shows degradation paths for specimens at the 1250 cm^{-1} FTIR peak, 306 nm nominal bandpass filter midpoint, 25% RH and at 3 different temperatures. Figure 3 shows the

13

effect of temperature on degradation. As expected, specimens exposed to higher temperatures tend to degrade faster than those at same conditions and lower temperatures.

5.2 Humidity Effects

Relationships between degradation rate and humidity are more complicated. Different chemical reactions respond differently to humidity and therefore damage degradation paths for each FTIR peak will relate in an individual manner to humidity. In our initial efforts to find an appropriate model for the humidity effect presented here, our approach is more empirical than scientifically based. NIST researches do, however, have initial hypotheses on the reasons for the observed behaviors and we expect that these will be used in subsequent modeling efforts.

Figure 4 has linear axes for humidity and logarithmic axes for the acceleration factor, plotted relative to 0%RH. As seen in Figure 4 (for the 1250 cm^{-1} FTIR peak), the NIST data suggest that the degradation rate decreases linearly as a function of relative humidity. Similar relationships are apparent in the all of the other FTIR peaks.
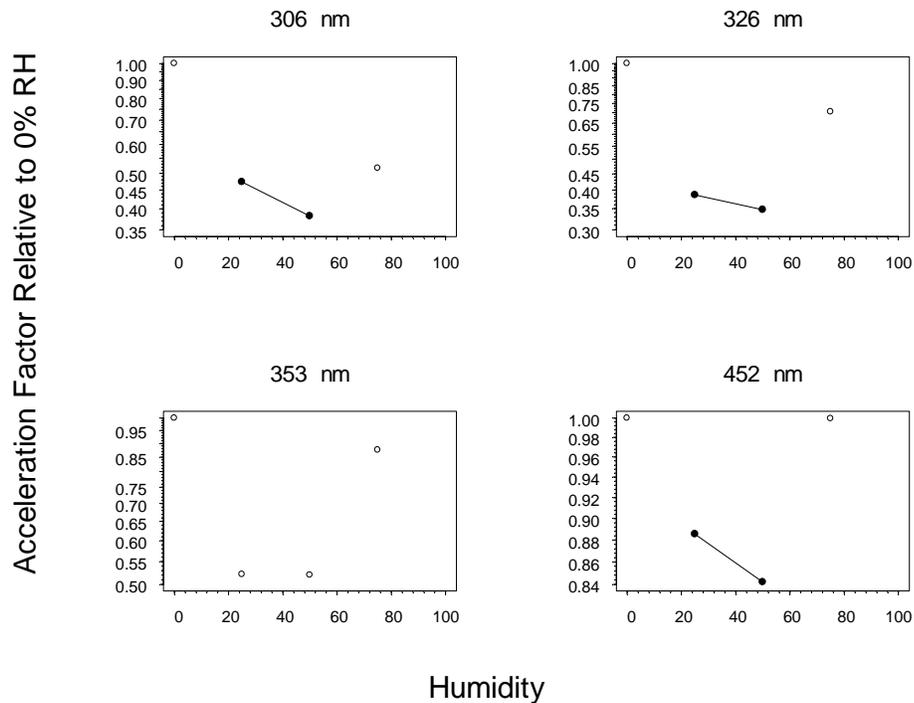

Figure 4 Indication of linear decreasing humidity effect for the 1250 cm^{-1} FTIR peak for specimens at 45°C

5.3 Overall Model and Bandpass Filter Approximation

Combining all of the model terms in equations (2) and (6), with

$$\mu = \beta_0 + \frac{E_a}{k_B \times \text{temp K}} - \beta_2 \times RH$$

we have

$$\log\big(d(t), CF, p\big) = \log\big[D_{\text{Tot}}(t)\big] + p \times \log(CF) \tag{7}$$

where

$$D_{\text{Tot}}(t) = \sum_{\lambda \text{ in the range on the BP filter}} \text{DOSAGE}_{\text{Tot}_\lambda} \times \phi(\lambda).$$

For the indoor data we have dosage over a range of a bandpass filters. For simplicity we assume a BP filter with rectangular shape over the given range for the filter. Therefore, $\text{DOSAGE}_{\text{Tot}_\lambda}$ corresponds to the value of the reported dosage divided by the range of the filter, giving the approximate dosage for the 2nm intervals that correspond to the outdoor data.

The parameters β_0, β_1, for the QQY relationship, E_a and β_2 are characteristic of the material and the degradation process and in our modeling we used $p = 1$ because there was no evidence against reciprocity. As a typical example, Figure 5 shows fitted lines for the proposed overall model for one response and experimental condition: the 1250 cm^{-1} FTIR peak, for specimens exposed under the 306 nm BP filter and 25%RH. The fit between the data points and the fitted model is good, considering the broadness of the response surface model. Deviations from the model are on the same order as the unit-to-unit experimental error when units were exposed at different times. We had similar results for other combinations of damage number, bandpass filter, and humidity.
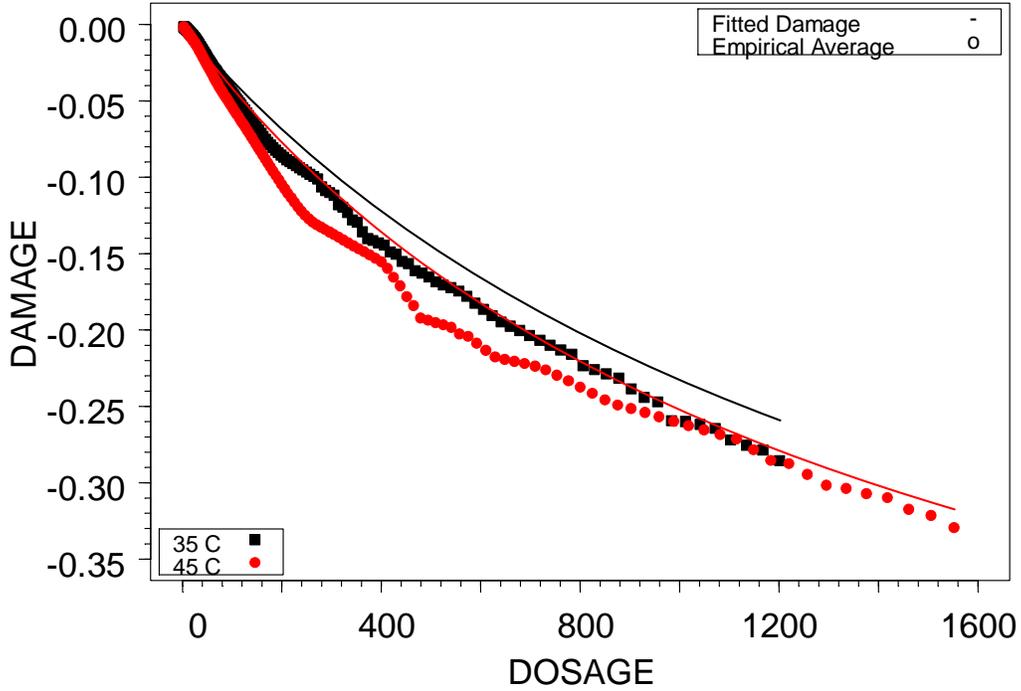
Figure 5 Indoor Data versus the Fitted Model for the 1250cm^{-1} FTIR peak, for specimens exposed under the 306 nm BP filter and 25%RH

6. Predictive Form of the Cumulative Damage Model

6.1 Cumulative Damage in a Time-Varying Environment

This section outlines the model that we used to predict total cumulative damage $Đ(t)$ as a function of a given environmental time series realization $\xi(\tau)$. The main difference in the predictive model is that the environmental variables can be allowed to vary with time. For a given environmental profile $\xi(\tau)$, the cumulative damage at time t for a particular unit can be expressed as

$$Đ(t) = \int_0^t \frac{dĐ[\tau, \xi(\tau)]}{\tau} \, d\tau \tag{8}$$

where $\xi(\tau) = [D_{Inst}(\tau), temp(\tau), RH(\tau)]$.

16

6.2 Evaluation Total Damage in a Time-Varying Environment

The integral in (8) is reasonably easy to compute after appropriate discretization of the time axis. The environmental data that we will use is reported at 12-minute intervals. Thus equation (8) will be computed with a summation in which the environmental conditions will be constant over each 12-minute period of time. Missing environmental data can be replaced by using a simple interpolation scheme.

For the cumulative damage model given in equation (1), the derivative of the cumulative damage with respect to dosage $d(t)$ is

$$g'(t) = \frac{d\text{Đ}[\tau, \xi(\tau)]}{d(t)} = \frac{1}{d(t) \times \sigma} [\text{Đ}(\infty) - \text{Đ}(0)] \left[\frac{\exp(z)}{(1 + \exp(z))^2} \right] \qquad (9)$$

where z is as defined in equation (2) and $d(t)$ is defined in equation (7), with estimates used to replace the unknown parameters. Then the prediction equation for the cumulative amount of damage at time t, based on the incremental values of dosage is:

$$Dosage_{CUM}(t) = \sum_{i=0}^{t} \Delta d(i)$$

$$Damage_{CUM}(t) = \sum_{i=0}^{t} \Delta\text{Đ}(i) \qquad (10)$$

where $\Delta d(t) = d(t) - d(t-1)$ and $\Delta\text{Đ}(t) = g'(t) * \Delta d(t)$

To test the predictive model, first we apply it to predict cumulative damage observed in the indoor data (constant environmental conditions). As expected and as shown in Figure 6, the predictions from the incremental model correspond almost exactly with the fitted model and agree well with the indoor data that were obtained under a controlled environment. Although this is a useful check, it is not proof of model adequacy because we are comparing the predictions against the same data that where used to build the model.
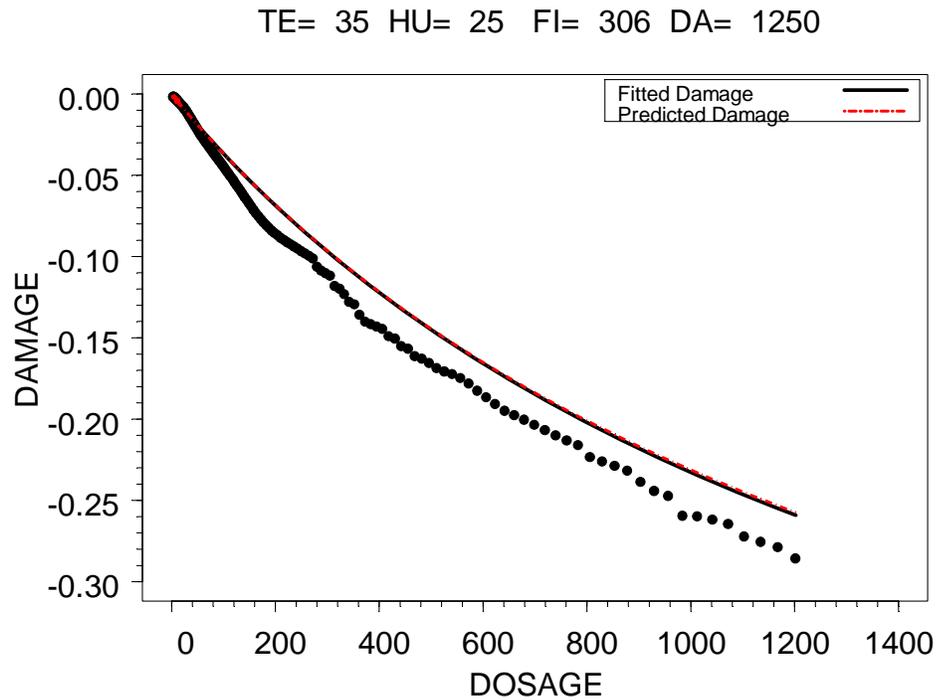
TE= 35 HU= 25 FI= 306 DA= 1250

Figure 6 Comparison of the overall fitted model and the predictions for the 1250cm^{-1} FTIR peak, for specimens exposed at 306 nm nominal bandpass filter midpoint, 35°C, and 25%RH

6.3 Prediction in a Time-Varying Environment

In this section we use our predictive model in (10) to predict the damage observed in the outdoor exposure chambers to check our ability to use a model estimated from indoor data to predict outdoor damage. We computed such predictions corresponding to all of the units that were tested in outdoor chambers at NIST. Here we show a few typical examples.

Our predictive model uses indoor data to estimate parameters of the model, as well as outdoor information about spectral dosage (every 2nm), humidity and temperature. Figure 7 uses lines to depict predictions for damage for different FTIR peaks for outdoor exposure group 18. The solid symbols represent the actual outdoor observations for the same group. For all four FTIR peaks, the different specimens agree well in terms of accumulated damage, as a function of dosage.
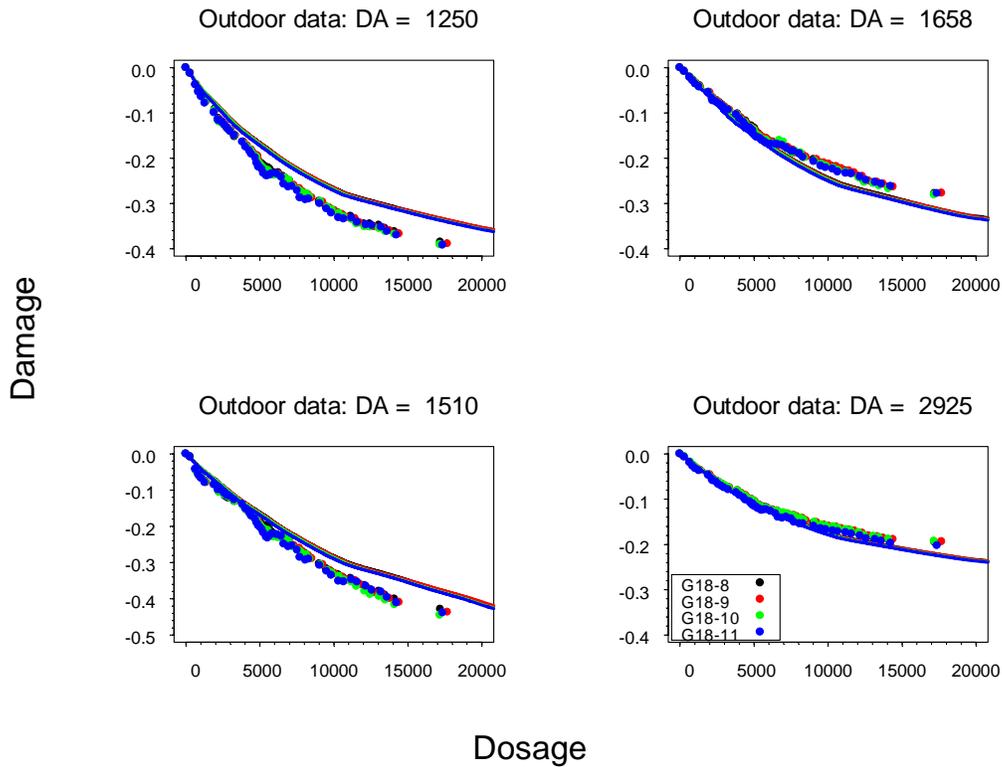
Figure 7 Comparison of the predictions for the outdoor specimens "G18-8", "G18-9","G18-10","G18-11" that were exposed at same time

Each plot in Figure 8 shows damage versus dosage for four specimens from outdoor exposure groups G1, G2, G3, and G4. Each of these groups began exposure at different points in time during 2002. Variability between observations of different groups is more apparent in this plot than what we see in Figure 7 because specimens began outdoors exposure at different points in time. That is, variability among these specimens is larger than what we see in Figure 7, due to different weather conditions during the different periods of exposure.
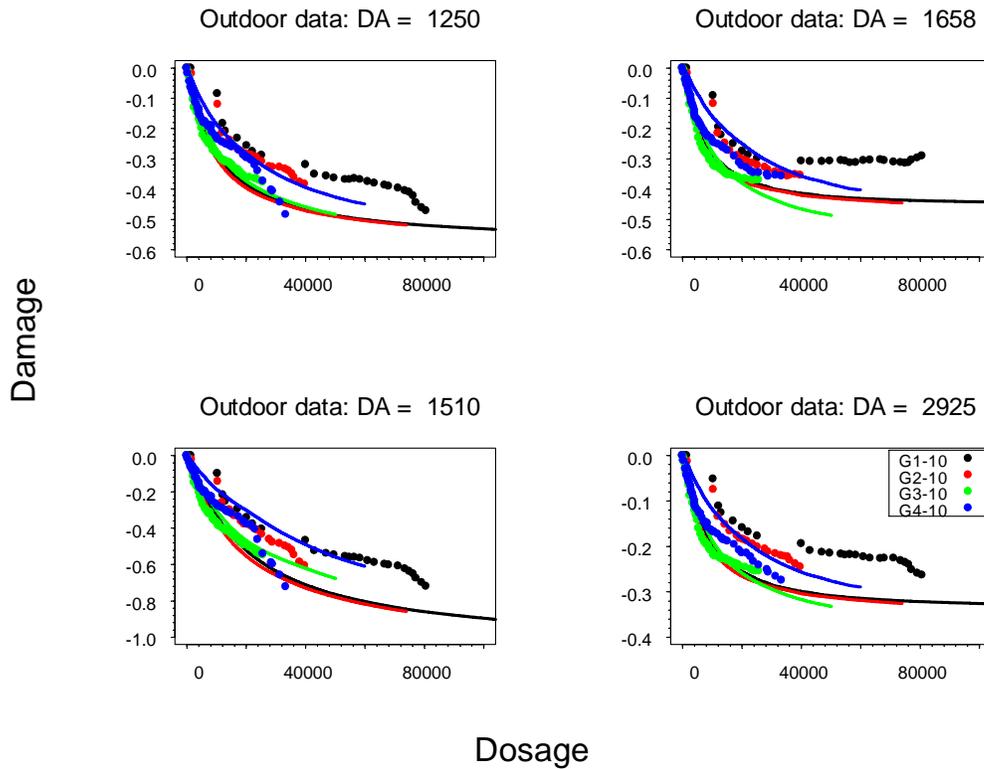
Figure 8 Comparison of predictions for the outdoor specimens "G1-10", "G2-10","G3-10","G4-10" that started exposure at different times

7. Concluding Remarks

This paper describes the methodology that we have developed to use indoor accelerated test data to find a model to describe the effect that environmental variables have on degradation rates. We have used this model to predict degradation rates and cumulative degradation in a time-varying environment, using outdoor weather data to drive the model. The variation between the predictions and the actual outdoor data is similar to the variability that we see in actual outdoor data.

8. Acknowledgments

References

- Blum, H. F. (1959), *Carcinogenesis by Ultraviolet Light.* Princeton University Press: Princeton, N.J.

- Chin, J. W.; Martin, J. W.; Embree, E. J.; Byrd, W. E. (2000) Use of Integrating Spheres as Uniform Sources for Accelerated UV Weathering of Advanced Materials. *Proceedings. American Chemical Society (ACS) Division of Polymeric Materials: Science and Engineering.* August 20-24, 2000, Washington, DC, American Chemical Society, Washington, DC, pages 145-146.

- Gillen, K. T., and Mead, K. E. (1980), "Predicting Life Expectancy and Simulating Age of Complex Equipment Using Accelerated Aging Techniques." Available from the National Technical Information Service, U. S. Department of Commerce, 5285 Port Royal Road, Springfield, VA 22151.

- James, T.H., Editor (1977), *The Theory of the Photographic Process*, 4th edition. Macmillan: New York.

- Joyce, W. B., Liou, K-Y., Nash, F. R., Bossard, P. R., and Hartman, R. L. (1985), *"Methodology of Accelerated Aging,"* AT&T Technical Journal, 64, 717–764.

- Kaetzel, L.J. (2001) Data Management and Spectral Solar UV Network, Service Life Prediction Methodologies and Metrologies, J.W. Martin and D.R. Bauer (Eds), American Chemical Society Symposium Series 805, p. 89.

- Martin, J. W. (1999). A Systems Approach to the Service Life Prediction Problem for Coating Systems. In D. R. Bauer and J. W. Martin, (Eds) *A Systems Approach to Service Life Prediction of Organic Coatings*, American Chemical Society: Washington.

- Martin, J. W., Saunders, S. C., Floyd, F. L., and Wineburg, J. P. (1996), *Methodologies for predicting the service lives of coating systems*. Federation of Societies for Coatings Technology: Blue Bell, PA.

- Meeker, W. Q., and Escobar, L. A. (1998), *Statistical Methods for Reliability Data*. John Wiley & Sons: New York.

- Nelson, W. (1990). *Accelerated Testing: Statistical Models, Test Plans, and Data Analyses*. John Wiley & Sons: New York.

- Starke, E. A., et al. (1996), Accelerated Aging of Materials and Structures, Publication NMAB-479, Washington DC: National Academy Press.

- Wernstøahl, K. M., and Carlsson, B. (1997) "Durability Assessment of Automotive Coatings—Design and Evaluation of Accelerated Tests," *Journal of Coatings Technology*, 69, 69-75.